



Searches for charged-lepton-flavor violation in $\chi_{bJ}(1P)$ decays

M. Abumusabh , I. Adachi , A. Aggarwal , L. Aggarwal , H. Ahmed , Y. Ahn , H. Aihara , N. Akopov ,
 S. Alghamdi , M. Alhakami , A. Aloisio , N. Alhubiti , K. Amos , M. Angelsmark , N. Anh Ky ,
 C. Antonioli , D. M. Asner , H. Atmacan , T. Aushev , R. Ayad , V. Babu , H. Bae , N. K. Baghel ,
 S. Bahinipati , P. Bambade , Sw. Banerjee , M. Barrett , M. Bartl , J. Baudot , A. Baur , A. Beaubien ,
 F. Becherer , J. Becker , J. V. Bennett , F. U. Bernlochner , V. Bertacchi , M. Bertemes , E. Bertholet ,
 M. Bessner , S. Bettarini , V. Bhardwaj , F. Bianchi , T. Bilka , D. Biswas , A. Bobrov , D. Bodrov ,
 A. Bondar , G. Bonvicini , J. Borah , A. Boschetti , A. Bozek , M. Bračko , P. Branchini ,
 R. A. Briere , T. E. Browder , A. Budano , S. Bussino , Q. Campagna , M. Campajola , L. Cao ,
 G. Casarosa , C. Cecchi , M.-C. Chang , P. Chang , P. Cheema , L. Chen , B. G. Cheon , C. Cheshta ,
 H. Chetri , K. Chilikin , K. Chirapatpimol , H.-E. Cho , K. Cho , S.-J. Cho , S.-K. Choi ,
 S. Choudhury , S. Chutia , J. Cochran , J. A. Colorado-Caicedo , I. Consigny , L. Corona , J. X. Cui ,
 E. De La Cruz-Burelo , S. A. De La Motte , G. De Nardo , G. De Pietro , R. de Sangro , M. Destefanis ,
 S. Dey , R. Dhayal , A. Di Canto , J. Dingfelder , Z. Doležal , I. Domínguez Jiménez , T. V. Dong ,
 X. Dong , G. Dujany , P. Ecker , D. Epifanov , J. Eppelt , R. Farkas , P. Feichtinger , T. Ferber ,
 T. Fillinger , C. Finck , G. Finocchiaro , F. Forti , A. Frey , B. G. Fulsom , A. Gabrielli , A. Gale ,
 E. Ganiev , M. Garcia-Hernandez , R. Garg , G. Gaudino , V. Gaur , V. Gautam , A. Gellrich ,
 G. Ghevondyan , R. Giordano , A. Giri , P. Gironella Gironell , B. Gobbo , R. Godang , P. Goldenzweig ,
 W. Gradl , E. Graziani , D. Greenwald , Y. Guan , K. Gudkova , I. Haide , Y. Han , H. Hayashii ,
 S. Hazra , M. T. Hedges , A. Heidelberg , G. Heine , I. Heredia de la Cruz , M. Hernández Villanueva ,
 T. Higuchi , M. Hoek , M. Hohmann , R. Hoppe , P. Horak , X. T. Hou , C.-L. Hsu , T. Humair ,
 T. Iijima , K. Inami , G. Inguglia , N. Ipsita , A. Ishikawa , R. Itoh , M. Iwasaki , P. Jackson , D. Jacobi ,
 W. W. Jacobs , E.-J. Jang , Q. P. Ji , S. Jia , Y. Jin , A. Johnson , J. Kandra , K. H. Kang , S. Kang ,
 G. Karyan , F. Keil , C. Ketter , C. Kiesling , D. Y. Kim , H. Kim , J.-Y. Kim , K.-H. Kim , H. Kindo ,
 K. Kinoshita , P. Kodyš , T. Koga , S. Kohani , A. Korobov , S. Korpar , E. Kovalenko , R. Kowalewski ,
 P. Križan , P. Krokovny , T. Kuhr , Y. Kullii , D. Kumar , J. Kumar , R. Kumar , K. Kumara ,
 T. Kunigo , A. Kuzmin , Y.-J. Kwon , S. Lacaprara , T. Lam , J. S. Lange , T. S. Lau , M. Laurenza ,
 R. Lebourder , F. R. Le Diberder , H. Lee , M. J. Lee , C. Lemettais , P. Leo , P. M. Lewis , C. Li ,
 H.-J. Li , L. K. Li , Q. M. Li , W. Z. Li , Y. Li , Y. B. Li , Y. P. Liao , J. Libby , J. Lin , S. Lin ,
 M. H. Liu , Q. Y. Liu , Y. Liu , Z. Liu , D. Liventsev , S. Longo , A. Lozar , T. Lueck , C. Lyu ,
 J. L. Ma , Y. Ma , M. Maggiora , S. P. Maharana , R. Maiti , G. Mancinelli , R. Manfredi , E. Manoni ,
 M. Mantovano , D. Marcantonio , S. Marcello , M. Marfoli , C. Marinas , C. Martellini , A. Martens ,
 T. Martinov , L. Massaccesi , M. Masuda , D. Matvienko , S. K. Maurya , M. Maushart , J. A. McKenna ,
 Z. Mednankin Gruberová , R. Mehta , F. Meier , D. Meleshko , M. Merola , C. Miller , M. Mirra ,
 K. Miyabayashi , H. Miyake , R. Mizuk , G. B. Mohanty , S. Moneta , A. L. Moreira de Carvalho ,
 H.-G. Moser , Th. Muller , R. Mussa , I. Nakamura , M. Nakao , H. Nakazawa , Y. Nakazawa , M. Naruki ,
 Z. Natkaniec , A. Natochii , M. Nayak , M. Neu , M. Niiyama , S. Nishida , R. Nomaru , S. Ogawa ,
 R. Okubo , H. Ono , F. Otani , P. Pakhlov , G. Pakhlova , A. Panta , S. Pardi , K. Parham , J. Park ,
 K. Park , S.-H. Park , A. Passeri , S. Patra , S. Paul , T. K. Pedlar , R. Pestotnik , M. Piccolo ,
 L. E. Piilonen , P. L. M. Podesta-Lerma , T. Podobnik , A. Prakash , C. Praz , S. Prell , M. T. Prim ,
 H. Purwar , P. Rados , S. Raiz , K. Ravindran , J. U. Rehman , M. Reif , S. Reiter , L. Reuter ,
 D. Ricalde Herrmann , I. Ripp-Baudot , G. Rizzo , S. H. Robertson , J. M. Roney , A. Rostomyan ,
 N. Rout , S. Saha , L. Salutari , D. A. Sanders , S. Sandilya , L. Santelj , C. Santos , V. Savinov ,
 B. Scavino , S. Schneider , G. Schnell , K. Schoenning , C. Schwanda , Y. Seino , K. Senyo , J. Serrano ,
 M. E. Seviar , C. Sfienti , W. Shan , G. Sharma , C. P. Shen , X. D. Shi , T. Shillington , T. Shimasaki 

J.-G. Shiu , D. Shtol , A. Sibidanov , F. Simon , J. Skorupa , R. J. Sobie , M. Sobotzik , A. Soffer ,
A. Sokolov , E. Solovieva , W. Song , S. Spataro , K. Špenko , B. Spruck , M. Starič , P. Stavroulakis ,
S. Stefkova , R. Stroili , M. Sumihama , N. Suwonjandee , M. Takahashi , M. Takizawa , U. Tamponi ,
S. S. Tang , K. Tanida , F. Tenchini , F. Testa , A. Thaller , T. Tien Manh , O. Tittel , R. Tiwary ,
E. Torassa , K. Trabelsi , F. F. Trantou , I. Tsaklidis , I. Ueda , K. Unger , Y. Unno , K. Uno , S. Uno ,
P. Urquijo , Y. Ushiroda , Y. V. Usov , S. E. Vahsen , R. van Tonder , K. E. Varvell , M. Veronesi ,
V. S. Vismaya , L. Vitale , V. Vobbilisetti , R. Volpe , M. Wakai , S. Wallner , M.-Z. Wang ,
A. Warburton , M. Watanabe , S. Watanuki , C. Wessel , E. Won , X. P. Xu , B. D. Yabsley ,
W. Yan , W. Yan , J. Yelton , K. Yi , J. H. Yin , K. Yoshihara , J. Yuan , Y. Yusa , L. Zani ,
F. Zeng , M. Zeyrek , B. Zhang , V. Zhilich , J. S. Zhou , Q. D. Zhou , L. Zhu , and R. Žlebčík

(The Belle and Belle II Collaborations)

We report the first searches for charged-lepton-flavor violation in decays of $\chi_{bJ}(1P)$ ($J = 0, 1,$ and 2) to a pair of charged leptons using 158 million $\Upsilon(2S)$ decays collected with the Belle detector in e^+e^- collisions at the KEKB collider. No significant signal is observed, and we set upper limits on the branching fractions for $\chi_{bJ}(1P)$ decays to $e^\pm\mu^\mp$ at the level of 10^{-6} and to $e^\pm\tau^\mp$ or $\mu^\pm\tau^\mp$ at the level of 10^{-5} . Limits on $\chi_{b0}(1P)$ decays are translated into bounds on the corresponding Wilson coefficients of scalar operators that mediate charged-lepton-flavor violation.

PACS numbers: 11.30.Hv, 12.60.-i, 13.20.Gd, 13.25.Gv, 14.60.-z

Charged-lepton-flavor violation (CLFV) is an unambiguous signature of physics beyond the standard model (SM) [1–3]. Extensive searches for CLFV in decays of the τ lepton [4, 5], mesons [6, 7], and the Higgs boson [8, 9] have placed stringent limits on new interactions. CLFV has so far been searched for in decays of pseudoscalar mesons like π^0 [10] and η [11] and vector quarkonia such as J/ψ [12] and $\Upsilon(nS)$ [13–16].

In this Letter, we report the first searches for CLFV in $\chi_{bJ}(1P)$ decays with $J = 0, 1,$ and 2 . The $\chi_{b0}(1P)$ decays provide a unique low-energy probe of CLFV in the scalar sector, complementary to direct searches for CLFV in Higgs boson decays. Similarly, the $\chi_{b1}(1P)$ and $\chi_{b2}(1P)$ decays provide the first searches for CLFV in decays of axial-vector and tensor particles, respectively [17]. Although not expected within the SM, interactions beyond the SM can induce $\chi_{bJ}(1P) \rightarrow \ell_1^+\ell_2^-$ with $\ell_1 \neq \ell_2$ and $\ell_1, \ell_2 = e, \mu, \tau$ [18] at experimentally observable rates [17], providing strong motivation for these searches. The observation of any such decay would clearly indicate the presence of new particles and interactions beyond the SM.

The $\chi_{bJ}(1P)$ states are copiously produced via $\Upsilon(2S) \rightarrow \gamma\chi_{bJ}(1P)$ in e^+e^- collisions. This study uses a sample of $(158 \pm 4) \times 10^6$ $\Upsilon(2S)$ mesons [19], the largest collected to date, produced in 24.7 fb^{-1} of data recorded by the Belle detector [20, 21] at a center-of-mass energy of 10.023 GeV [22] at the KEKB collider [23, 24].

Several decays are simulated to estimate reconstruction efficiencies and background contributions. We simulate $\Upsilon(2S)$ decays using EVTGEN [25], leptonic $\chi_{bJ}(1P)$ decays using the multi-body phase-space decay model, radiative decays using the helicity-amplitude decay model, and leptonic $\Upsilon(1S)$ decays using the

vector-meson-to-dilepton decay model. Processes such as $e^+e^- \rightarrow \ell^+\ell^-$, $q\bar{q}$ ($q = u, d, s, c$), $\gamma\gamma$, and $\gamma q\bar{q}$ that potentially contribute to backgrounds are simulated using PYTHIA 6.4 [26]. We use PHOTOS [27] to simulate final-state radiation and GEANT3 [28] to model the response of the Belle detector.

To characterize background rates, estimate systematic uncertainties, and validate our analysis procedure, we study cascade decays of $\chi_{bJ}(1P) \rightarrow \gamma\Upsilon(1S)$ with subsequent $\Upsilon(1S) \rightarrow e^+e^-$ or $\Upsilon(1S) \rightarrow \mu^+\mu^-$ decays as our control modes. These control modes are chosen because direct decays of $\chi_{bJ}(1P)$ to same-flavor lepton pairs proceed via two photons or the Higgs boson in the SM, and have branching fractions of $\mathcal{O}(10^{-20})$ – $\mathcal{O}(10^{-9})$ [29], making them unmeasurable. In the searches for $\chi_{bJ}(1P) \rightarrow e^\pm\tau^\mp$ or $\mu^\pm\tau^\mp$, we reconstruct the $\tau^- \rightarrow \mu^-\bar{\nu}_\mu\nu_\tau$ and $\tau^- \rightarrow e^-\bar{\nu}_e\nu_\tau$ decay modes, respectively, to minimize backgrounds from $e^+e^- \rightarrow \ell^+\ell^-$ events, where $\ell = e, \mu$.

We select events with exactly two oppositely charged tracks, one identified as an electron and the other as a muon. Each track is required to have a momentum greater than 200 MeV [30] and a distance of closest approach to the e^+e^- collision point of less than 4.5 cm along the e^- beam direction and 1.5 cm in the plane transverse to it. A track is identified as an electron if its electron likelihood ratio exceeds 0.5 ; otherwise, it is identified as a muon when its muon likelihood ratio exceeds 0.9 . The efficiencies of this selection are 92.4% and 93.8% for electrons and muons, respectively [31, 32]. We recover the energy that an electron may lose to bremsstrahlung by adding to its four-momentum the four-momenta of photon candidates found within 60 mrad of its momentum. To make the datasets mutually exclusive, we require the momenta of electrons or muons from $\chi_{bJ}(1P)$

decays exceed 3.5 GeV and that from τ decays fall below 3.5 GeV.

All photons must have energies above 50 MeV to reduce the contamination from beam background. The energies of the photons from $\Upsilon(2S) \rightarrow \gamma\chi_{bJ}(1P)$ and $\chi_{bJ}(1P) \rightarrow \gamma\Upsilon(1S)$ decays, labeled E_{γ_1} and E_{γ_2} , respectively, are known to mostly satisfy the relation $E_{\gamma_1} < E_{\gamma_2}$ [33, 34]. To reduce combinatorial background, we require $E_{\gamma_1} < 250$ MeV and $E_{\gamma_2} > 250$ MeV.

For the $\chi_{bJ}(1P) \rightarrow e^\pm\mu^\mp$ decays and the control modes, a four-constraint kinematic fit is performed using energy-momentum conservation and the measured uncertainties of the final-state momenta. Kinematically inconsistent events are suppressed by a loose requirement on the fit χ^2 value, $\chi_{4C}^2 < 1000$, a selection that retains nearly all signal decays.

The control mode $\chi_{bJ}(1P) \rightarrow \gamma e^+e^-$ is mimicked by the radiative Bhabha process, whose cross section is significantly larger than that for $\Upsilon(2S)$ production. A veto that rejected 99% of Bhabha events was applied during data taking [35]. To further suppress such events, we remove regions dominated by Bhabha backgrounds, characterized by $\theta_{e^-} < 0.75$ rad and $\theta_{\gamma_1} < 0.6$ rad, or $\theta_{\gamma_1} > 2.2$ rad, where θ_{e^-} and θ_{γ_1} are the angles of the final-state electron and the γ_1 candidate with respect to the electron beam. Additionally, we reject any event with an e^- track with momentum above 6.4 GeV. We estimate the efficiency of the control mode using events that pass a dedicated simulation of the Bhabha veto.

In terms of the total energy E_X and momentum \vec{p}_X of a set of particles X , the mass recoiling against that set is given by

$$M_X^{\text{recoil}} = \sqrt{(E_{e^+e^-} - E_X)^2 - (\vec{p}_{e^+e^-} - \vec{p}_X)^2}, \quad (1)$$

where $E_{e^+e^-}$ and $\vec{p}_{e^+e^-}$ are the total energy and momentum of the colliding electron and positron. Control events are required to have $M_{\gamma_1\gamma_2}^{\text{recoil}}$ in [9.43, 9.51] GeV, encompassing the $\Upsilon(1S)$ resonance. Both control and signal events are required to have $M_{\gamma_1}^{\text{recoil}}$ in [9.81, 9.95] GeV, covering the $\chi_{bJ}(1P)$ states. Also, we require $M_{\gamma_1\ell_1}^{\text{recoil}}$ to be in [0.6, 2.8] GeV for $\chi_{bJ}(1P) \rightarrow \ell_1^\pm\tau^\mp$ searches, where ℓ_1 refers to the higher-energy lepton in the final state.

In 40% of events, multiple $\Upsilon(2S)$ candidates are formed due to photons from beam background and final-state radiation. For $\chi_{bJ}(1P) \rightarrow e^\pm\mu^\mp$ and the control modes, we retain the candidate with the lowest χ_{4C}^2 , which selects the true candidate 98% of the time in simulation. For $\chi_{bJ}(1P) \rightarrow \ell_1^\pm\tau^\mp$, we retain the candidate whose γ_1 energy yields an $M_{\gamma_1\ell_1}^{\text{recoil}}$ value closest to the known τ mass [36], selecting the true candidate 75% of the time. These best-candidate selections do not bias the analysis results.

To obtain the yields of the control modes $N_{J,\ell\ell}$, we perform unbinned maximum-likelihood fits to $M_{\gamma_1}^{\text{recoil}}$ distributions separately for $\gamma\gamma e^+e^-$ and $\gamma\gamma\mu^+\mu^-$ candidates.

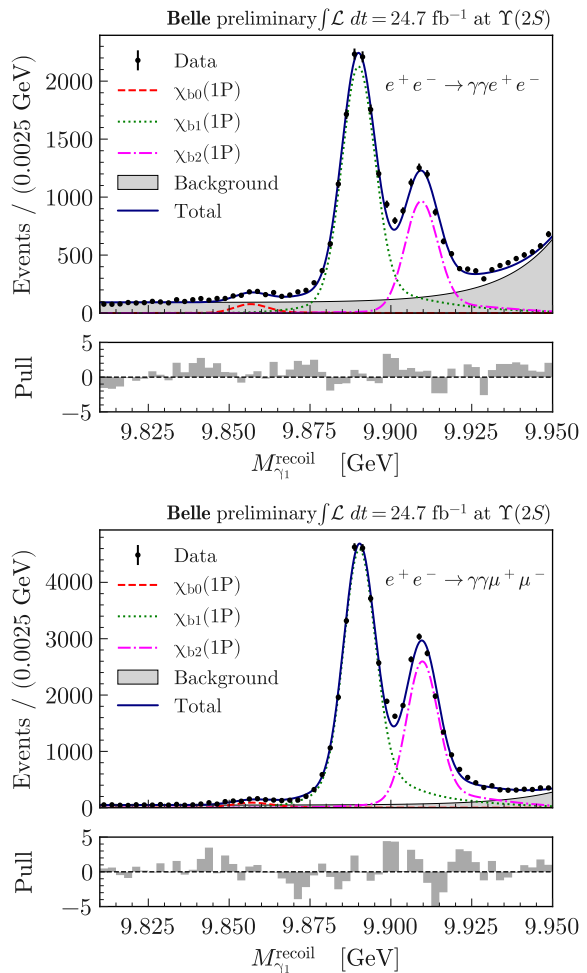


FIG. 1. $M_{\gamma_1}^{\text{recoil}}$ distributions for $e^+e^- \rightarrow \gamma\gamma e^+e^-$ (top) and $e^+e^- \rightarrow \gamma\gamma\mu^+\mu^-$ (bottom) overlaid with fit results.

For both, we model the probability density function (PDF) for each $\chi_{bJ}(1P)$ as a sum of two Gaussian functions and a bifurcated Gaussian function, all sharing a common central value. The central value and the widths of the PDF for $\chi_{b1}(1P)$ are determined by the fit to data, while the parameters for the $\chi_{b0}(1P)$ and $\chi_{b2}(1P)$ components are fixed with respect to them. We model each background distribution as the sum of an exponential PDF and a constant PDF. Figure 1 shows the distributions of $M_{\gamma_1}^{\text{recoil}}$ with the fitted PDF components overlaid. From each $N_{J,\ell\ell}$, we calculate the product of branching fractions for $\Upsilon(2S) \rightarrow \gamma\chi_{bJ}(1P)$, $\chi_{bJ}(1P) \rightarrow \gamma\Upsilon(1S)$, and $\Upsilon(1S) \rightarrow \ell^+\ell^-$ as

$$\mathcal{B}(\Upsilon(2S) \rightarrow \gamma\gamma\ell^+\ell^-) = \frac{N_{J,\ell\ell}}{N_{\Upsilon(2S)}\epsilon_{J,\ell\ell}}, \quad (2)$$

where $N_{\Upsilon(2S)}$ is the number of $\Upsilon(2S)$ mesons in the data, and $\epsilon_{J,\ell\ell}$ is the efficiency to reconstruct $\Upsilon(2S) \rightarrow \gamma\gamma\ell^+\ell^-$ via $\chi_{bJ}(1P)$. The efficiencies for $\gamma\gamma e^+e^-$ are 16%, 16%,

and 13% for $J = 0, 1$, and 2, respectively; for $\gamma\gamma\mu^+\mu^-$ they are 28%, 30%, and 29%, respectively. Table I summarizes the results, which agree with the products of the world averages of the individual branching fractions in $\Upsilon(2S) \rightarrow \gamma\gamma\ell^+\ell^-$ [37].

Decay	$\Upsilon(2S) \rightarrow \gamma\gamma e^+e^-$	$\Upsilon(2S) \rightarrow \gamma\gamma\mu^+\mu^-$
$J = 0$	0.175 ± 0.018	0.147 ± 0.010
$J = 1$	5.179 ± 0.056	5.912 ± 0.041
$J = 2$	2.799 ± 0.058	3.267 ± 0.037

TABLE I: Products of branching fractions in units of 10^{-4} for $\Upsilon(2S) \rightarrow \gamma\chi_{bJ}(1P)$, $\chi_{bJ}(1P) \rightarrow \gamma\Upsilon(1S)$ and $\Upsilon(1S) \rightarrow \ell^+\ell^-$ measured in the control modes. Uncertainties are statistical only.

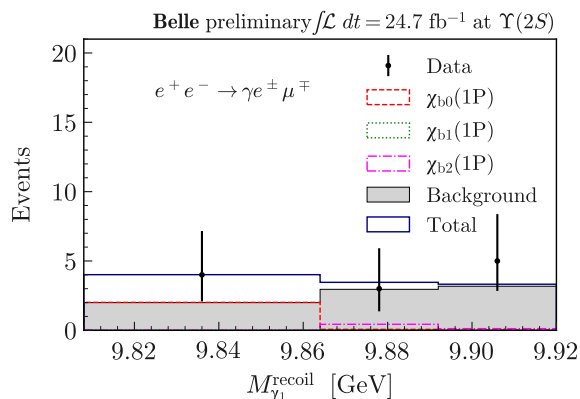


FIG. 2. $M_{\gamma_1}^{\text{recoil}}$ distribution for $e^+e^- \rightarrow \gamma e^+\mu^+$ candidates. The $\chi_{b1}(1P)$ component is too small to be visible.

To extract the signal yields for $\chi_{bJ}(1P) \rightarrow e^\pm\mu^\mp$, we perform a maximum-likelihood fit to the $M_{\gamma_1}^{\text{recoil}}$ distribution, dividing the signal region into three bins. Histogram templates for signal components and background are estimated from simulations. We float the yields of signal components, while the background normalization is constrained by three nuisance parameters describing the systematic uncertainty in each bin. Figure 2 shows the distribution of $M_{\gamma_1}^{\text{recoil}}$ for $\gamma e^\pm\mu^\mp$ candidates in data along with the fitted signal and background components.

For $\chi_{bJ}(1P) \rightarrow \ell^\pm\tau^\mp$, an unbinned maximum-likelihood fit has been performed to the $M_{\gamma_1}^{\text{recoil}}$ and $M_{\gamma_1\ell_1}^{\text{recoil}}$ distributions simultaneously. For both $M_{\gamma_1}^{\text{recoil}}$ and $M_{\gamma_1\ell_1}^{\text{recoil}}$, we use the same signal models as for $M_{\gamma_1}^{\text{recoil}}$ in the control modes, with the central values and widths of the signal components fixed to values determined from simulation and corrected by the differences observed between simulation and data in the control modes. We model the background distribution in $M_{\gamma_1}^{\text{recoil}}$ using the background PDF of the control modes and the background distribution in $M_{\gamma_1\ell_1}^{\text{recoil}}$ with an exponential func-

tion. Figure 3 shows the $M_{\gamma_1}^{\text{recoil}}$ and $M_{\gamma_1\ell_1}^{\text{recoil}}$ distributions for $\gamma e^\pm\tau^\mp$ and $\gamma\mu^\pm\tau^\mp$ candidates in data and the results of the fits.

We include systematic uncertainties from the calibration of track-finding, lepton identification, photon detection, and trigger efficiencies, which are corrected in simulation to match the data. The track-finding systematic uncertainties are 0.35% per track [21]. Lepton-identification systematic uncertainties are estimated using control samples of $J/\psi \rightarrow \ell\ell$ and $\gamma\gamma \rightarrow \mu^+\mu^-$ [31, 32]. The photon detection efficiency uncertainties are estimated using radiative Bhabha events. Trigger systematic uncertainties are estimated to be 1%, based on the efficiencies of independent sub-triggers for $e^+e^- \rightarrow \gamma\gamma e^+e^-$ and $e^+e^- \rightarrow \gamma\gamma\mu^+\mu^-$ events. We also include uncertainties from values fixed in the fit PDFs, branching fractions [37], efficiencies from simulation, and $N_{\Upsilon(2S)}$. Table II lists all systematic uncertainties and their quadrature sums for each channel.

The branching fraction $\mathcal{B}(\chi_{bJ}(1P) \rightarrow \ell_1\ell_2)$ is obtained from the number of signal events $N_{J,\ell_1\ell_2}$ using

$$\mathcal{B}(\chi_{bJ}(1P) \rightarrow \ell_1\ell_2) = \frac{N_{J,\ell_1\ell_2}/N_{\Upsilon(2S)}}{\mathcal{B}(\Upsilon(2S) \rightarrow \gamma\chi_{bJ}(1P))\epsilon_{J,\ell_1\ell_2}}. \quad (3)$$

Here $\epsilon_{J,\ell_1\ell_2}$ is the efficiency to reconstruct $\gamma\ell_1^\pm\ell_2^\mp$ via the $\chi_{bJ}(1P)$, including the relevant τ branching fractions.

As all signal yields are consistent with zero, we calculate upper limits on branching fractions using the CLs method [38]. For $\chi_{bJ}(1P) \rightarrow e^\pm\mu^\mp$, we use `pyhf` [39] and for $\chi_{bJ}(1P) \rightarrow \ell^\pm\tau^\mp$, we use a frequentist calculator from `Roostats` [40]. In each case, an ensemble of 5000 pseudo-experiments is used. Systematic uncertainties are included by smearing the yields. Table III lists the efficiencies, branching fractions, and upper limits on them at the 90% confidence level, as well as the correlation coefficients C_{mn} from simultaneous fits to all three spin states, where $m, n = 0, 1, 2$.

The Wilson coefficients for the left- and right-handed scalar operators $C_{\text{SL}}^{q\ell_1\ell_2}$ and $C_{\text{SR}}^{q\ell_1\ell_2}$ that mediate CLFV are constrained by the branching fractions for $\chi_{b0}(1P)$ decays, relative to the energy scale Λ of the new interaction [17], using the following equation:

$$\left(\frac{C_{\text{SL}}^{q\ell_1\ell_2}}{\Lambda^2}\right)^2 + \left(\frac{C_{\text{SR}}^{q\ell_1\ell_2}}{\Lambda^2}\right)^2 = \frac{16\pi m_\chi \Gamma_\chi \mathcal{B}(\chi \rightarrow \ell_1\ell_2)}{G_{\text{F}}^2 f_\chi^2 m_b^2 m_{\ell_2}^2 (m_\chi^2 - m_{\ell_2}^2)^2}. \quad (4)$$

Here G_{F} is the Fermi constant, m_b is the bottom-quark mass, m_{ℓ_2} is the heavier lepton mass, and m_χ is the mass of $\chi_{b0}(1P)$, which are obtained from Ref. [37]. To estimate the total decay width of the $\chi_{b0}(1P)$, we divide the predicted partial decay width of $\chi_{b0}(1P) \rightarrow \gamma\Upsilon(1S)$ [41] by its measured branching fraction [37], yielding $\Gamma_\chi = 1.23 \pm 0.17$ MeV. The decay constant f_χ is obtained from Ref. [42]. We include the uncertainties on f_χ and Γ_χ by smearing the results. From Table III, we obtain bounds

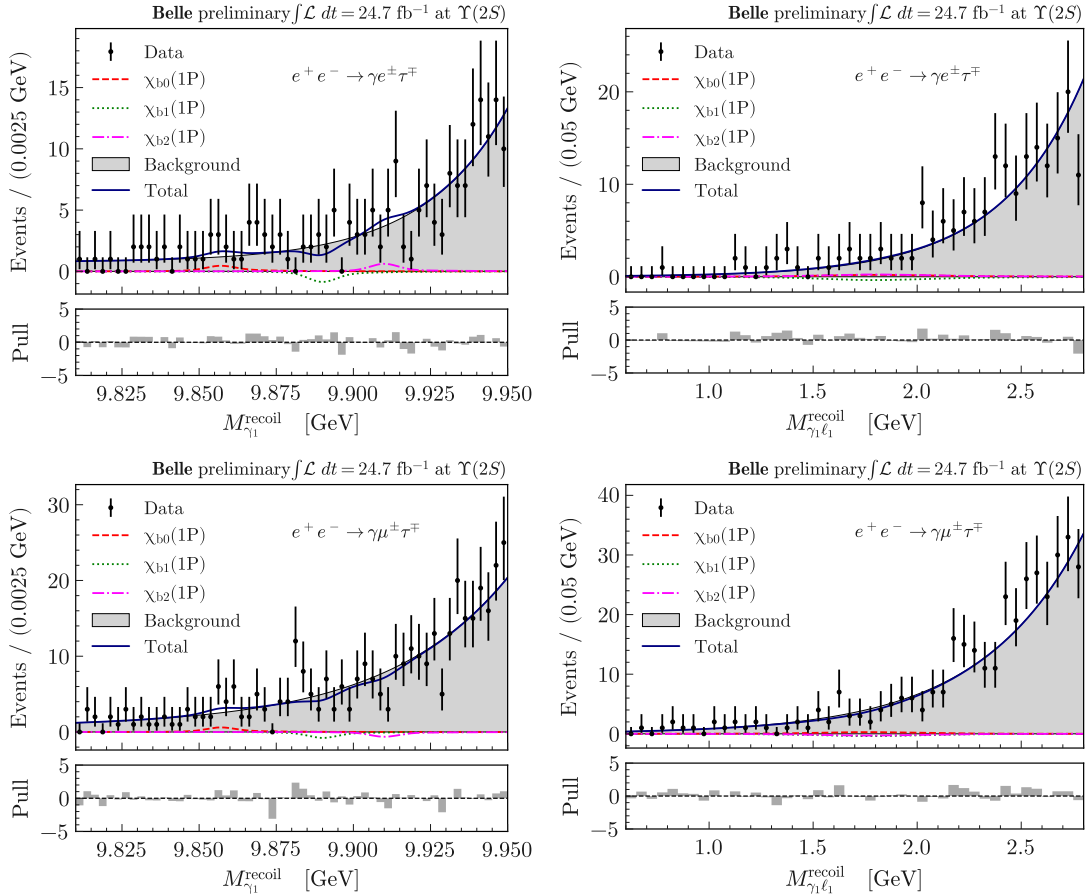


FIG. 3. Fit projections of $M_{\gamma_1}^{\text{recoil}}$ (left) and $M_{\gamma_1 \ell_1}^{\text{recoil}}$ (right) for $e^+e^- \rightarrow \gamma e^\pm \tau^\mp$ (top row) $e^+e^- \rightarrow \gamma \mu^\pm \tau^\mp$ (bottom row).

Source	Systematic uncertainties (in %)		
	$e^\pm \mu^\mp$	$e^\pm \tau^\mp$	$\mu^\pm \tau^\mp$
$N_{\Upsilon(2S)}$	2.3	2.3	2.3
Track finding	0.7	0.7	0.7
Lepton identification	1.9, 2.0, 2.0	2.2	2.0
Photon detection	2.0	2.0	2.0
Trigger	1.0	1.0	1.0
PDF parameters	-	1.1, 0.4, $^{+1.8}_{-1.2}$	1.1, 0.4, $^{+1.8}_{-1.2}$
Simulation statistics	0.1	0.1	0.1
Control modes	19.9, 10.0, 10.0	19.9, 10.0, 10.0	19.9, 10.0, 10.0
Total	20.3, 10.7, 10.7	20.3, 10.7, 10.8	20.3, 10.7, 10.8

TABLE II: Systematic uncertainties, where three numbers when listed correspond to $J = 0, 1$, and 2 , respectively.

Decay	$J = 0$			$J = 1$			$J = 2$			Correlation coefficients		
	ϵ	BR	UL	ϵ	BR	UL	ϵ	BR	UL	C_{01}	C_{12}	C_{20}
$\chi_{bJ}(1P) \rightarrow e^\pm \mu^\mp$	28.7	1.2 ± 1.3	4.0	31.2	0.0 ± 1.3	1.5	29.9	0.2 ± 0.8	1.8	-0.0065	-4.1	-0.51
$\chi_{bJ}(1P) \rightarrow e^\pm \tau^\mp$	20.8	14.0 ± 18.0	41.0	21.4	-13.0 ± 8.0	13.0	20.4	9.0 ± 12.0	26.0	-6.0	5.3	-33.0
$\chi_{bJ}(1P) \rightarrow \mu^\pm \tau^\mp$	31.9	11.0 ± 10.0	28.0	33.7	-8.0 ± 5.0	9.0	31.5	-6.0 ± 5.0	9.0	5.3	8.2	4.2

TABLE III: Efficiencies (ϵ) in %, branching fractions (BR) and upper limits (UL) at the 90% confidence level in units of 10^{-6} , and correlation coefficients (C_{mn} , where $m, n = 0, 1, 2$) in % from simultaneous fits to all three spin states.

at the 90% confidence level on these Wilson coefficients, as shown by the circles in Figure 4. The regions outside the circles are excluded by the obtained results.

In summary, we present the first searches for CLFV in all nine possible final states with $\ell_1 \neq \ell_2$ and $\ell_1, \ell_2 = e, \mu, \tau$ in $\chi_{bJ}(1P)$ decays ($J = 0, 1, 2$), and constrain the Wilson coefficients of previously unexplored scalar operators mediating CLFV.

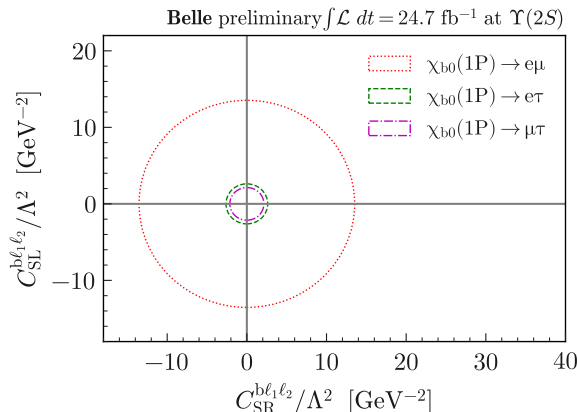


FIG. 4. Upper limits at the 90% confidence level on Wilson coefficients of scalar operators that mediate CLFV.

We thank A. Petrov for insightful discussions. This work, based on data collected using the Belle detector, which was operated until June 2010, was supported by the Ministry of Education, Culture, Sports, Science, and Technology (MEXT) of Japan, the Japan Society for the Promotion of Science (JSPS), and the Tau-Lepton Physics Research Center of Nagoya University; the Australian Research Council including grants DP210101900, DP210102831, DE220100462, LE210100098, LE230100085; Austrian Federal Ministry of Education, Science and Research (FWF) and FWF Austrian Science Fund No. P 31361-N36; National Key R&D Program of China under Contract No. 2022YFA1601903, National Natural Science Foundation of China and research grants No. 11575017, No. 11761141009, No. 11705209, No. 11975076, No. 12135005, No. 12150004, No. 12161141008, and No. 12175041, and Shandong Provincial Natural Science Foundation Project ZR2022JQ02; the Czech Science Foundation Grant No. 22-18469S; Horizon 2020 ERC Advanced Grant No. 884719 and ERC Starting Grant No. 947006 “InterLeptons” (European Union); the Carl Zeiss Foundation, the Deutsche Forschungsgemeinschaft, the Excellence Cluster Universe, and the VolkswagenStiftung; the Department of Atomic Energy (Project Identification No. RTI 4002), the Department of Science and Technology of India, and the UPES (India) SEED finding programs Nos. UPES/R&D-SEED-INFRA/17052023/01 and

UPES/R&D-SOE/20062022/06; the Istituto Nazionale di Fisica Nucleare of Italy; National Research Foundation (NRF) of Korea Grants No. 2021R1-A6A1A-03043957, No. 2021R1-F1A-1064008, No. 2022R1-A2C-1003993, No. 2022R1-A2C-1092335, No. RS-2016-NR017151, No. RS-2018-NR031074, No. RS-2021-NR060129, No. RS-2023-00208693, No. RS-2024-00354342 and No. RS-2025-02219521, Radiation Science Research Institute, Foreign Large-Size Research Facility Application Supporting project, the Global Science Experimental Data Hub Center, the Korea Institute of Science and Technology Information (K25L2M2C3) and KREONET/GLORIAD; the Polish Ministry of Science and Higher Education and the National Science Center; the Ministry of Science and Higher Education of the Russian Federation and the HSE University Basic Research Program, Moscow; University of Tabuk research grants S-1440-0321, S-0256-1438, and S-0280-1439 (Saudi Arabia); the Slovenian Research Agency Grant Nos. J1-50010 and P1-0135; Ikerbasque, Basque Foundation for Science, and the State Agency for Research of the Spanish Ministry of Science and Innovation through Grant No. PID2022-136510NB-C33 (Spain); the Swiss National Science Foundation; the Ministry of Education and the National Science and Technology Council of Taiwan; and the United States Department of Energy and the National Science Foundation. These acknowledgements are not to be interpreted as an endorsement of any statement made by any of our institutes, funding agencies, governments, or their representatives. We thank the KEKB group for the excellent operation of the accelerator; the KEK cryogenics group for the efficient operation of the solenoid; and the KEK computer group and the Pacific Northwest National Laboratory (PNNL) Environmental Molecular Sciences Laboratory (EMSL) computing group for strong computing support; and the National Institute of Informatics, and Science Information NETwork 6 (SINET6) for valuable network support.

-
- [1] M. Raidal *et al.*, *Eur. Phys. J. C* **57**, 13 (2008), arXiv:0801.1826 [hep-ph].
 - [2] A. de Gouvea and P. Vogel, *Prog. Part. Nucl. Phys.* **71**, 75 (2013), arXiv:1303.4097 [hep-ph].
 - [3] A. Celis, V. Cirigliano, and E. Passemar, *Phys. Rev. D* **89**, 095014 (2014), arXiv:1403.5781 [hep-ph].
 - [4] B. Aubert *et al.* (BaBar), *Phys. Rev. Lett.* **104**, 021802 (2010), arXiv:0908.2381 [hep-ex].
 - [5] K. Uno *et al.* (Belle), *JHEP* **10**, 19 (2021), arXiv:2103.12994 [hep-ex].
 - [6] R. Alonso, B. Grinstein, and J. Martin Camalich, *JHEP* **10**, 184 (2015), arXiv:1505.05164 [hep-ph].
 - [7] A. Abada, D. Bečirević, M. Lucente, and O. Sumensari, *Phys. Rev. D* **91**, 113013 (2015), arXiv:1503.04159 [hep-ph].

- [8] A. M. Sirunyan *et al.* (CMS), Phys. Rev. D **104**, 032013 (2021), arXiv:2105.03007 [hep-ex].
- [9] G. Aad *et al.* (ATLAS), JHEP **07**, 166 (2023), arXiv:2302.05225 [hep-ex].
- [10] E. Cortina Gil *et al.* (NA62), Phys. Rev. Lett. **127**, 131802 (2021), arXiv:2105.06759 [hep-ex].
- [11] D. B. White *et al.*, Phys. Rev. D **53**, 6658 (1996).
- [12] M. Ablikim *et al.* (BESIII), Phys. Rev. D **103**, 112007 (2021), arXiv:2103.11540 [hep-ex].
- [13] J. P. Lees *et al.* (BaBar), Phys. Rev. Lett. **104**, 151802 (2010), arXiv:1001.1883 [hep-ex].
- [14] J. P. Lees *et al.* (BaBar), Phys. Rev. Lett. **128**, 091804 (2022), arXiv:2109.03364 [hep-ex].
- [15] S. Patra *et al.* (Belle), JHEP **2022**, 095 (2022), arXiv:2201.09620 [hep-ex].
- [16] R. Dhamija *et al.* (Belle), JHEP **02**, 187 (2024), arXiv:2309.02739 [hep-ex].
- [17] D. E. Hazard and A. A. Petrov, Phys. Rev. D **94**, 074023 (2016), arXiv:1607.00815 [hep-ph].
- [18] Charge-conjugate decay modes are implied throughout.
- [19] X. L. Wang *et al.* (Belle), Phys. Rev. D **84**, 071107 (2011), arXiv:1008.1774.
- [20] A. Abashian *et al.* (Belle), Nucl. Instrum. Meth. A **479**, 117 (2002).
- [21] J. Brodzicka *et al.* (Belle), PTEP **2012**, 04D001 (2012), arXiv:1212.5342 [hep-ex].
- [22] Natural units ($\hbar = c = 1$) are used throughout this Letter.
- [23] S. Kurokawa and E. Kikutani, Nucl. Instrum. Meth. A **499**, 1 (2003).
- [24] T. Abe *et al.*, PTEP **2013**, 03A001 (2013).
- [25] D. J. Lange, Nucl. Instrum. Meth. A **462**, 152 (2001).
- [26] T. Sjstrand, S. Mrenna, and P. Skands, JHEP **2006**, 026 (2006).
- [27] E. Barberio and Z. Was, Comput. Phys. Commun. **79**, 291 (1994).
- [28] R. Brun, F. Bruyant, M. Maire, A. C. McPherson, and P. Zancarini, (1987), CERN Report No. DD/EE/84-1.
- [29] S. Godfrey and H. E. Logan, Phys. Rev. D **93**, 055014 (2016), arXiv:1510.04659 [hep-ph].
- [30] All variables are defined in the laboratory frame, unless otherwise mentioned.
- [31] K. Hanagaki, H. Kakuno, H. Ikeda, T. Iijima, and T. Tsukamoto, Nucl. Instrum. Meth. A **485**, 490 (2002), arXiv:hep-ex/0108044.
- [32] A. Abashian *et al.*, Nucl. Instrum. Meth. A **491**, 69 (2002).
- [33] M. Kornicer *et al.* (CLEO), Phys. Rev. D **83**, 054003 (2011), arXiv:1012.0589 [hep-ex].
- [34] J. P. Lees *et al.* (BaBar), Phys. Rev. D **90**, 112010 (2014), arXiv:1410.3902 [hep-ex].
- [35] B. Cheon *et al.*, Nucl. Instrum. Meth. A **494**, 548 (2002).
- [36] I. Adachi *et al.* (Belle II), Phys. Rev. D **108**, 032006 (2023), arXiv:2305.19116 [hep-ex].
- [37] S. Navas *et al.* (Particle Data Group), Phys. Rev. D **110**, 030001 (2024).
- [38] G. Cowan, K. Cranmer, E. Gross, and O. Vitells, Eur. Phys. J. C **71**, 1554 (2011), arXiv:1007.1727 [physics.data-an].
- [39] L. Heinrich, M. Feickert, G. Stark, and K. Cranmer, J. Open Source Softw. **6**, 2823 (2021).
- [40] L. Moneta *et al.*, PoS **ACAT2010**, 057 (2010), arXiv:1009.1003 [physics.data-an].
- [41] S. Godfrey and K. Moats, Phys. Rev. D **92**, 054034 (2015).
- [42] H. S. Chung, JHEP **09**, 195 (2021), arXiv:2106.15514 [hep-ph].